Supporting information for

Sequential backbone assignment based on dipolar amide-to-amide correlation experiments

ShengQi Xiang†, Kristof Grohe†, Petra Rovó, Suresh Kumar Vasa, Karin Giller, Stefan Becker, and Rasmus Linser[a,*]

[a]Department for NMR-based Structural Biology, Max Planck Institute for Biophysical Chemistry, Göttingen, Germany.

†The authors contributed equally.

*corresponding author: rali@nmr.mpibpc.mpg.de

Details on solid-state NMR acquisition parameters:

CP contact times of 2.5 ms, 400 µs, and 9 ms and effective fields of 18.3 kHz/44.8 kHz (80-100 % ramp on ^{13}C), 18.8 kHz/41.3 kHz (80-100 % ramp on ^{15}N), and 43.6 kHz/16.4 kHz (80-100 % ramp on ^{13}C) were used for ^{1}H^{N}/^{13}C, ^{1}H^{N}/^{15}N, and ^{13}C/^{15}N transfers, respectively. ^{13}CO/^{13}CA transfers were achieved by the HORROR condition with a 9 ms spin lock on CA at an effective field of 25.2 kHz. Decoupling fields were set to 2.9 kHz on ^{15}N and 5 kHz on ^{1}H. Recycle delays were set to 500 ms. The total experimental time for each experiment is listed in Table S1. The acquisition parameters are listed in Table S2. Apodization of the each dimension was achieved with a squared sine bell window function shifted by 90°.

Spectrum	Total experimental time
(H)CANH	32 h 13 min
(H)CA(CO)NH	15 h25 min
(H)CONH	15 h 2 min
(H)CO(CA)NH	15 h 23 min
H(N)(CO)(CA)NH	33 h
(H)N(CO)(CA)NH	33 h

Table S1. Experimental time for each experiment.

	^{13}CO	^{13}CA	^{15}N	$^{1}H^{N}$ (indirect)	$^{1}H^{N}$ (direct)
Spectral width (kHz)	1.9	4.5	2.6	4.0	30
Acquisition time (ms)	8.67	3.53	14.3	9.0	40
Number of Data points	42	90	74	72	1920

Table S2. Acquisition parameters.

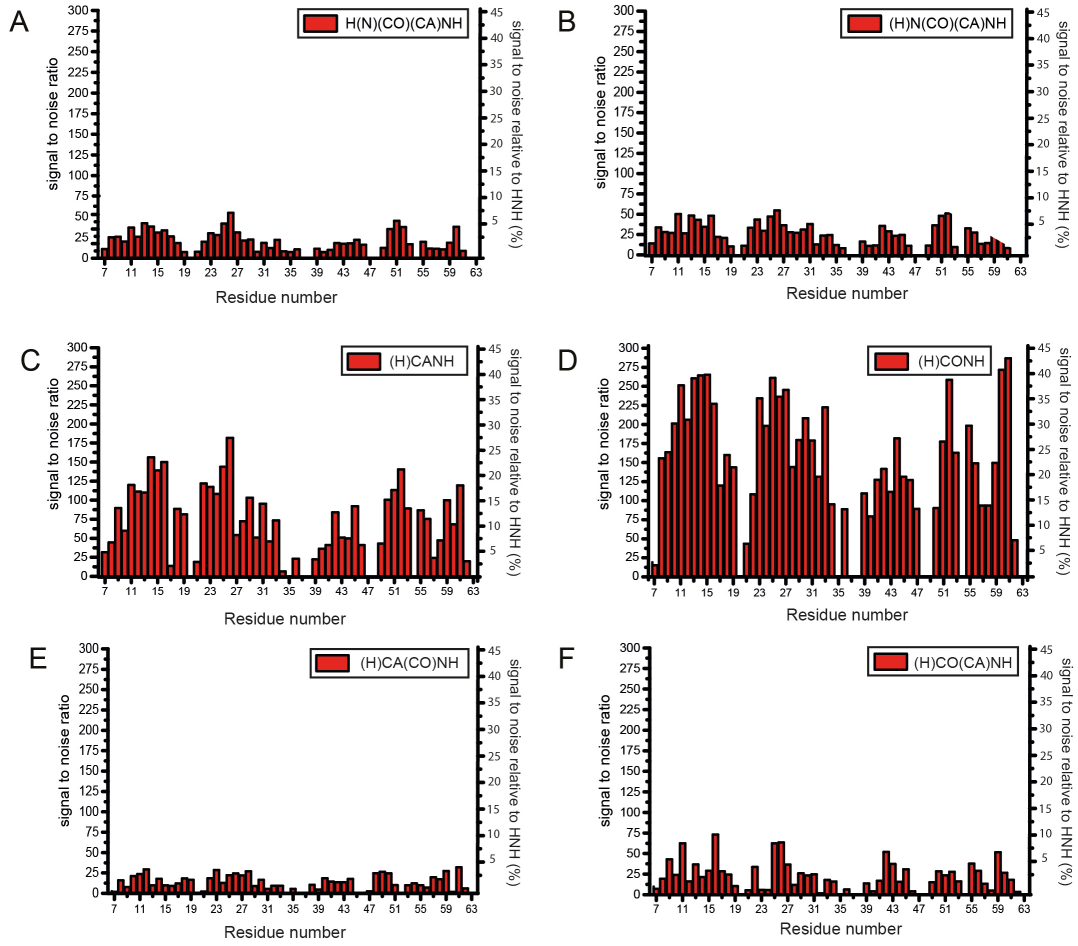

Fig. S1. Signal to noise ratios of A) H(N)(CO)(CA)NH (sequential peak), B) (H)N(CO)(CA)NH (sequential peak), C) (H)CANH, D) (H)CONH, E) (H)CA(CO)NH, F) (H)CO(CA)NH spectra as a function of residue number. The sensitivity values were read out using peak heights as obtained by CCPNmr (Vranken et al. 2005) and were scaled according to the experimental time (see Supporting Table 2). The right scale relates the s/n axis on the left again to the (H)NH sensitivity as a standard measure. Given the fact that usually 1D (first-scan) spectra are used for such a comparison to avoid different processing and acquisition parameters for 2D and 3D experiments, the axis here is calculated from the 1D first-scan intensity ratio (see Figure 3 of the Main Manuscript, read out using Topspin) subjected to the average 3D peak height.

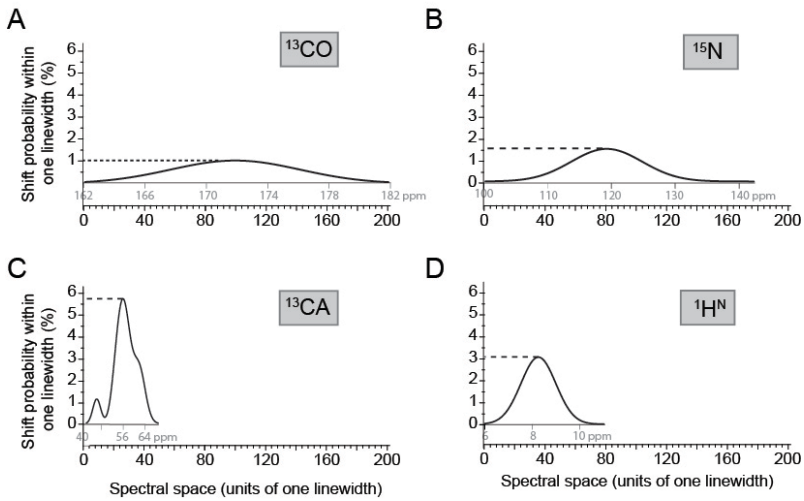

Fig. S2. BMRB data bank distributions of chemical shifts (in percent) over spectral space in units of one linewidth (FWHM) for ^{13}CO (A), ^{15}N (B), ^{13}CA (C), and ^{1}H^{N} (D) shifts as in Main Text Figure 5. Here, for ^{13}CO, ^{15}N, and the ^{1}H^{N}, we replotted the theoretical probabilities approximating the minimum obtainable (natural) linewidths, assuming 50 Hz for ^{1}H^{N}, 20 Hz for ^{15}N and ^{13}CO. The ^{13}CA lineshape will additionally be influenced by evolution of scalar couplings (triplet of 20 Hz to ^{2}H plus doublet of 35 Hz to ^{13}CB), thus this minimum linewidth is represented as 110 Hz.

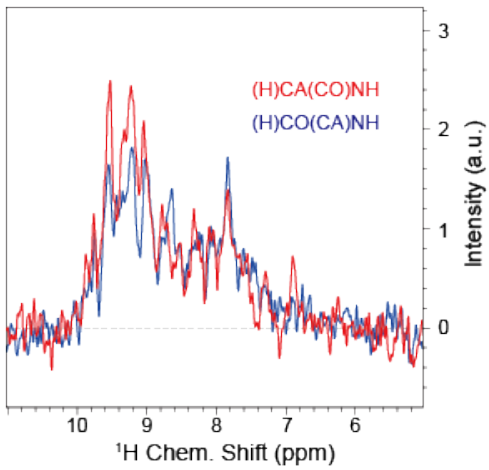

Fig. S3. Comparison between first FIDs of (H)CA(CO)NH and (H)CO(CA)NH. The latter provides slightly weaker signal to noise in the first scan. The (H)CO(CA)NH can potentially be replaced by the out-and-back (H)CO(CA)CONH experiment (Barbet-Massin et al. 2013), which may have advantages when shaped pulses are a bottleneck in the straight-through version.

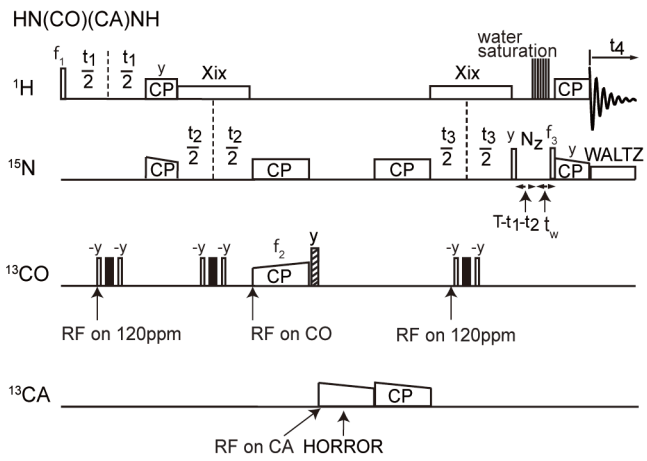

Fig. S4. Pulse program for a 4D HN(CO)(CA)NH experiment to obtain $^{1}H^{N}_{i}$, $^{15}N_{i}$, $^{1}H^{N}_{i+1}$ and $^{15}N_{i+1}$ correlations. Open, filled, and striped bars represent 90°, 180°, and trim pulses, respectively. The train of proton pulses for water saturation follows the MISSISSIPI approach (Zhou and Rienstra 2008). All other pulses were applied with phase x if not indicated explicitly. The phase cycle φ_1=x, -x; φ_2=4(+x), 4(-x); φ_3=x, x, -x, -x; φ_{rec}=x,-x,-x, x,-x, x, x,-x was employed.

Supporting Information references:

Barbet-Massin E et al. (2013) Out-and-back 13C-13C scalar transfers in protein resonance assignment by proton-detected solid-state NMR under ultra-fast MAS. J Biomol NMR 56:379-386

Vranken WF et al. (2005) The CCPN data model for NMR spectroscopy: development of a software pipeline. Proteins 59:687–696

Zhou DH, Rienstra CM (2008) High-Performance Solvent Suppression for Proton-Detected Solid-State NMR. J Magn Reson 192:167-172